

NASA TECHNICAL
MEMORANDUM

NASA TM X-53542

December 1, 1966

NASA TM X-53542

FACILITY FORM 602

<u>N67 14910</u> (ACCESSION NUMBER)	_____
<u>28</u> (PAGES)	_____ (THRU)
<u>TMX-53542</u> (NASA CR OR TMX OR AD NUMBER)	_____ (CODE)
	<u>31</u> (CATEGORY)

ORBITAL INVESTIGATION OF PROPELLANT DYNAMICS IN A
LARGE ROCKET BOOSTER

by H. J. BUCHANAN AND F. M. BUGG
Aero-Astroynamics Laboratory

GPO PRICE \$ _____

CFSTI PRICE(S) \$ _____

NASA

Hard copy (HC) 3.00

Microfiche (MF) .65

*George C. Marshall
Space Flight Center,
Huntsville, Alabama*

ff 653 July 65

TECHNICAL MEMORANDUM X-53542

ORBITAL INVESTIGATION OF PROPELLANT DYNAMICS
IN A LARGE ROCKET BOOSTER

By

H. J. Buchanan and F. M. Bugg

George C. Marshall Space Flight Center

Huntsville, Alabama

ABSTRACT

Experimental data on the dynamics of liquid hydrogen in the 6.6 m (260 in) diameter tank of an S-IVB stage during boost, at S-IVB stage cutoff, and in orbit are presented. For the boost phase of flight, the amplitude of the sloshing liquid decreased from approximately .25 m (10 in) at the beginning of S-IVB stage boost to a minimum of about .038 m (1.5 in) as the liquid level moved past the baffle. The frequency during the S-IVB stage engine burn increased from approximately .44 cycles per second to .70 cycles per second and showed good agreement with predicted values.

During orbital coast, periods of the liquid hydrogen oscillation were measured through a range of accelerations from $8.0 \times 10^{-5} g_0$ to $4.4 \times 10^{-4} g_0$. Period data taken while the acceleration was varying with time did not agree with either the predicted natural or coupled periods. Nearly steady-state conditions existed for the $8.0 \times 10^{-5} g_0$ acceleration and the 300 sec to 330 sec slosh periods measured at this acceleration were close to the predicted value of 315 sec. The good agreement between experiment and "high-g" theory (i.e., theory neglecting surface tension and contact angle effects) at this very low acceleration tends to verify the validity of Bond number as a criterion for defining "high-g" conditions with regard to liquid sloshing.

NASA - GEORGE C. MARSHALL SPACE FLIGHT CENTER

Technical Memorandum X-53542

ORBITAL INVESTIGATION OF PROPELLANT DYNAMICS
IN A LARGE ROCKET BOOSTER

By

H. J. Buchanan and F. M. Bugg

STRUCTURAL DYNAMICS SECTION
DYNAMICS ANALYSIS BRANCH
DYNAMICS AND FLIGHT MECHANICS DIVISION
AERO-ASTRODYNAMICS LABORATORY
RESEARCH AND DEVELOPMENT OPERATIONS

LIST OF ILLUSTRATIONS

<u>Figure</u>	<u>Title</u>	<u>Page</u>
1	Location of Thermocouples, Liquid-Vapor Sensor and Propellant Utilization Probe.....	8
2	Liquid Hydrogen Tank Dimensions.....	9
3	Slosh Amplitude and Predicted Damping During Second Stage Burn.....	10
4	Liquid Hydrogen Level During Second Stage Burn....	11
5	Sloshing Frequencies During Second Stage Burn.....	12
6	Acceleration During Second Stage Burn.....	13
7	Propellant Dynamics at Second Stage Cutoff.....	14
8	Accelerations During Orbit.....	15
9	Bond Numbers During Orbit.....	16
10	Comparison of Liquid-Vapor Sensor and Thermocouple Readings at One Location.....	17
11	Slosh Periods During Orbit.....	18
12	Propellant Level During Orbit.....	19

DEFINITION OF SYMBOLS

<u>Symbol</u>	<u>Definition</u>
h	liquid level, meters (inches) - measured from tank bottom
t'	second stage burn time, seconds
t	time after liftoff, seconds
a	longitudinal acceleration of vehicle
g ₀	9.8 m/sec ² (32.17 ft/sec ²)
ω	frequency, cycles/second
η	peak-to-peak amplitude, meters (inches)
ξ	damping ratio
τ	period, seconds
B ₀	Bond number, $ar^2/(\sigma/\rho)$
r	tank radius
σ	liquid surface tension
ρ	liquid density

TECHNICAL MEMORANDUM X-53542

ORBITAL INVESTIGATION OF PROPELLANT DYNAMICS IN A LARGE ROCKET BOOSTER

SUMMARY

Experimental data on the dynamics of liquid hydrogen in the 6.6 m (260 in) diameter tank of an S-IVB stage during boost, at S-IVB stage cutoff, and in orbit are presented. For the boost phase of flight, the amplitude of the sloshing liquid decreased from approximately .25 m (10 in) at the beginning of S-IVB stage boost to a minimum of about .038 m (1.5 in) as the liquid level moved past the baffle. The frequency during the S-IVB stage engine burn increased from approximately .44 cycles per second to .70 cycles per second and showed good agreement with predicted values.

During orbital coast, periods of the liquid hydrogen oscillation were measured through a range of accelerations from $8.0 \times 10^{-5} g_0$ to $4.4 \times 10^{-4} g_0$. Period data taken while the acceleration was varying with time did not agree with either the predicted natural or coupled periods. Nearly steady-state conditions existed for the $8.0 \times 10^{-5} g_0$ acceleration and the 300 sec to 330 sec slosh periods measured at this acceleration were close to the predicted value of 315 sec. The good agreement between experiment and "high-g" theory (i.e., theory neglecting surface tension and contact angle effects) at this very low acceleration tends to verify the validity of Bond number as a criterion for defining "high-g" conditions with regard to liquid sloshing.

I. INTRODUCTION

Space flights to the moon or further space explorations will have as mission profiles waiting orbits or other engine-off low gravity coast periods after which the engine must be restarted. To accomplish such flights, the propellant dynamics in low gravity must be understood and controlled. Propellant dynamics problems occur in the following phases of flight:

- (1) Boost
- (2) Engine cutoff (transition from high to low acceleration environment)
- (3) Orbit.

Several analytical investigations have been made of low gravity fluid dynamics (see refs. 1-4). Some experimental investigations have been made in which low gravity conditions were simulated in tests on the ground; the results of one of these are presented in reference 1. A Saturn IB liquid hydrogen orbital experiment has been performed to evaluate the hydrogen vent and engine restart systems of the S-IVB stage in an orbital environment (refs. 5-7). As a part of this experiment, data concerning the propellant (liquid hydrogen) dynamics in the S-IVB stage during boost, at S-IVB stage engine cutoff, and in orbit were obtained. These data are unique with regard to the tank size, acceleration range, and test duration for which they were obtained. This report presents these propellant dynamics data and compares them with the results of analytical investigations.

II. DISCUSSION

A. Apparatus

The experiment was conducted in an S-IVB stage which was launched July 5, 1966, by the Saturn IB flight designated AS-203. Figure 1 shows the S-IVB stage liquid hydrogen tank and the locations of the propellant utilization probe, thermocouples, and liquid-vapor sensor. The propellant utilization probe was a capacitance type of liquid level sensor designed to operate during the high acceleration of boost, but not to operate at the low acceleration levels in orbit. The thermocouples and liquid vapor sensor shown were those which gave propellant dynamics data in orbit. Figure 2 shows the overall dimensions of the tank, deflector, and baffle, and also the location of the television camera. The photographs in figure 7 show the portion of the tank viewed with the television and indicate that a large part of the tank wall was blocked from view by the deflector and baffle. The lines on the tank wall were .61 m (24 in) apart.

Detailed descriptions of the instrumentation can be found in reference 6. All data were telemetered to the ground.

B. Results

The propellant dynamics data from the liquid hydrogen orbital experiment are presented for the boost, injection, and orbit phases of the vehicle flight. In general, amplitudes and frequencies were measured for the sloshing liquid during boost and in orbit. The propellant reaction to the acceleration change at the second stage engine cutoff is presented based on visual data from video tape.

1. Boost

Propellant sloshing during boost must be minimized to keep control disturbances small and to prevent severe unsettling of the propellant at engine cutoff (during transition from the high acceleration of boost to the low acceleration environment of orbit). The S-IVB stage has a baffle installed to minimize this sloshing at the end of S-IVB first burn to eliminate or reduce the agitation of liquid due to transition from high to low acceleration. The data from the propellant utilization probe were used to determine the slosh amplitude at the probe and the frequency. The location of the maximum slosh amplitude was estimated from the television record and used with the assumption that the slosh wave was first mode to determine the maximum amplitude at the wall. Since no attenuation factor was used and since the location of maximum amplitude was estimated, the amplitude data are approximate. However, the video tape of the propellant during second stage boost tends to confirm that the amplitudes presented are correct.

The slosh amplitude at the probe and the maximum amplitude at the wall are presented in figure 3 with the damping predicted for the deflector and baffle. (The damping values are from reference 9.) Figure 3 shows a rapid decrease in slosh amplitude during the first 80 seconds of second stage boost, and minimum points in the amplitude curves at about 143 seconds and 265 seconds. Figure 4 shows that the liquid surface was in contact with the curved portion of the tank wall for approximately the first 80 seconds of second stage boost, and the surface was near the deflector and baffle when the minimum amplitudes occurred. During the last few seconds of second stage burn, while the liquid surface was below the baffle, a sharp increase in sloshing amplitude occurred. To prevent this amplitude build-up, the baffle should be located so that the liquid surface at cutoff is above and very near the baffle.

The frequency during second stage boost increased from approximately .44 cycles per second to .70 cycles per second as shown in figure 5. The predicted frequencies were in good agreement with these experimental values. The second stage acceleration, shown in figure 6, was used with high-g theory (ref. 8) to calculate the predicted natural and coupled slosh frequencies of figure 5. These accelerations are the preflight predicted values and are nearly the same as the accelerations which existed in flight.

2. Engine Cutoff

The kinetic energy in the sloshing propellant at the end of boosted flight is the main source of energy for the liquid dynamics at cutoff. As discussed in reference 9, this energy from boost slosh

can result in large amplitude sloshing or spraying of the liquid when the acceleration is drastically reduced, as at engine cutoff.

In the SA-203 flight second stage engine cutoff occurred at about 435.5 seconds after liftoff. Propulsive venting of the liquid oxygen tank, begun .2 second after cutoff, provided an acceleration of approximately $2.0 \times 10^{-4} g_0$ which tended to keep the liquid hydrogen in the tank bottom. The sequence of photographs in figure 7, taken from the video tape, shows part of the propellant dynamics at cutoff. At $t = 422$ seconds, the liquid surface appeared to be smooth and ripple-free so that the bottom of the liquid hydrogen tank was clearly visible. Shortly after cutoff, $t = 442$ seconds, the liquid surface was covered with small ripples. At $t = 474$ seconds a geyser of liquid was in view moving from left to right. At $t = 495$ seconds the liquid was returning to the tank bottom. The following observations were made from the video tape:

- (1) The liquid wetted the baffle two seconds after engine cutoff.
- (2) The liquid surface moved first to the left of the television view, then the geyser (shown in figure 7 at $t = 474$ seconds) came into view moving up and to the right. The geyser appeared to be above the deflector at 23 seconds after cutoff.
- (3) The upward movement of liquid stopped about 58 seconds after cutoff and the liquid from the geyser began to resettle.
- (4) At 157 seconds after cutoff, the propellant was again below the baffle and apparently settled in the tank bottom. Magnification of the slosh amplitude occurred as expected and was successfully controlled by the use of baffle, deflector and oxygen vent thrust.

3. Orbit

Knowledge of forces and moments exerted on an orbiting vehicle by the sloshing propellant is essential to the design of efficient attitude control systems. Propellant sloshing frequency and amplitude are important factors in determining these forces and moments. The acceleration, tank size, and propellant properties are among the factors which define slosh frequency.

Longitudinal acceleration of the orbiting S-IVB stage was provided primarily by propulsive venting of the oxygen and hydrogen tanks. A record of the longitudinal acceleration for the orbiting S-IVB is shown in figure 8. These accelerations, taken from reference 6, are computed values based on the vent nozzle characteristics and the properties of the vapor being vented. The acceleration spike near $t = 6000$ seconds in figure 8 was produced by a fuel lead, and the near zero acceleration at 11,000 seconds was achieved by closing the vents.

At the end of each orbit, as the vehicle was passing over the United States, a relatively large acceleration was imposed on the vehicle for a short period of time. This resulted in the series of smaller spikes shown in figure 8. Because of the shorter period associated with this higher acceleration, and the longer recording times afforded by the overlapping ground stations, most of the sloshing period measurements were taken during these spikes. Points at which the thermocouples and liquid-vapor sensors indicated slosh are indicated by the filled symbols.

The Bond number is a ratio of body forces to cohesive forces and is used in defining low gravity regimes. The Bond number variation with flight time is shown in figure 9. The tank radius was selected for the characteristic dimension. For the liquid hydrogen, a kinematic surface tension, σ/ρ , of approximately $26.76 \text{ cm}^3/\text{sec}^2$ was assumed. The resulting figure is similar to figure 8 from which the acceleration values were taken. In general, the Bond number was above 100 for most of the flight, and all measurements were made at Bond numbers greater than 300.

Figure 10 shows the output of a thermocouple and a liquid vapor sensor at a particular location. These curves are typical of those used to determine the sloshing periods.

The slosh periods measured during orbital coast are presented in figure 11 as a function of longitudinal acceleration, a/g_0 . For comparison, a theoretical natural period and a theoretical coupled period are shown. The natural period was calculated using the linear potential theory developed in reference 8 for tanks of arbitrary shape, and does not include the effects of surface tension, contact angle, or viscosity. Since for the Bond numbers under consideration, this theory gives essentially the same frequencies as the theory of Satterlee and Reynolds (ref. 2), which does include surface tension and contact angle, it was thought to be more accurate for this tank shape. The values for coupled period were obtained from a flight simulation which included the control system, the rigid body dynamics of the vehicle, and a spring-mass slosh model. This slosh model was also based on the linear potential theory of reference 8. A more detailed discussion of this analysis, including the equations used and some typical results, can be found in reference 9.

Together, figures 8 and 11 seem to indicate that the slosh frequency is strongly influenced by the time rate of change of longitudinal acceleration. Data taken for $d(a/g_0)/dt = 0$ exhibit very little scatter and match very closely the theoretical natural period. On the other hand, data for $d(a/g_0)/dt \neq 0$, showed much more scatter and indicated periods substantially shorter than either of the predictions. The usual procedure for slosh calculations, in general, has been to ignore the effect of $d(a/g_0)/dt$ and, as indicated in figure 5, this has proved to be adequate for the high-g case. Since, under low-g conditions, the fluid reacts more slowly, the frequency cannot change quickly enough to compensate for a rapidly changing longitudinal acceleration. The data presented here seem to show that for low-g calculations, this effect should be included. The good agreement between experiment and theory at $a/g_0 = 8.0 \times 10^{-5}$ in figure 11 tends to verify the importance of Bond number in defining "high-g" conditions with regard to liquid sloshing. The "high-g" theory of reference 9 (i.e., theory neglecting surface tension and contact angle effects) gave good predictions of sloshing period at these high Bond numbers even at this very low acceleration level.

The axial distances between thermocouple and mean liquid level (figure 12) for the thermocouples which gave period data varied from about .076 (3 in) to .56 m (22in). There was not, however, sufficient data to determine either the amplitude or direction of the sloshing motion. From the television record of the orbital flight, some motions of the liquid were discernible but, because the liquid at the tank wall was not in view, it was impossible to determine amplitudes or verify the period data.

CONCLUSIONS

For the boost phase of flight, the amplitude of the sloshing liquid decreased from approximately .25 m (10 in) at the beginning of S-IVB stage boost to a minimum of about .038 m (1.5 in) as the liquid level moved past the anti-slosh baffle. The frequency during the S-IVB stage engine burn increased from approximately .44 cycles per second to .70 cycles per second and showed good agreement with predicted values.

During orbital coast, periods of the liquid hydrogen oscillation were measured through a range of accelerations from $8.0 \times 10^{-5} g_0$ to $4.4 \times 10^{-4} g_0$. Period data taken while the acceleration was varying with time did not agree with either the predicted natural or coupled periods. Nearly steady-state conditions existed for the 8.0×10^{-5} acceleration, and the 300 second to 330 second slosh periods measured at this acceleration were close to the predicted value of 315 seconds.

The good agreement between experiment and "high-g" theory (i.e., theory neglecting surface tension and contact angle effects) at this very low acceleration tends to verify the importance of Bond number in defining "high-g" conditions with regard to liquid sloshing.

For verification of theory including the effects of surface tension and contact angle, experiments in low gravity and at low Bond number ($.1 < B_0 < 100$) are required. Experience gained in the present investigation would make it possible to locate the instrumentation in such a way that accurate measurements of amplitude and interface shape could be obtained in addition to the frequency data. If experimental verification of the low gravity analytical tools could be achieved, accurate predictions of the interaction of the vehicle control system - with propellant dynamics would be possible for all phases of future vehicle flights.

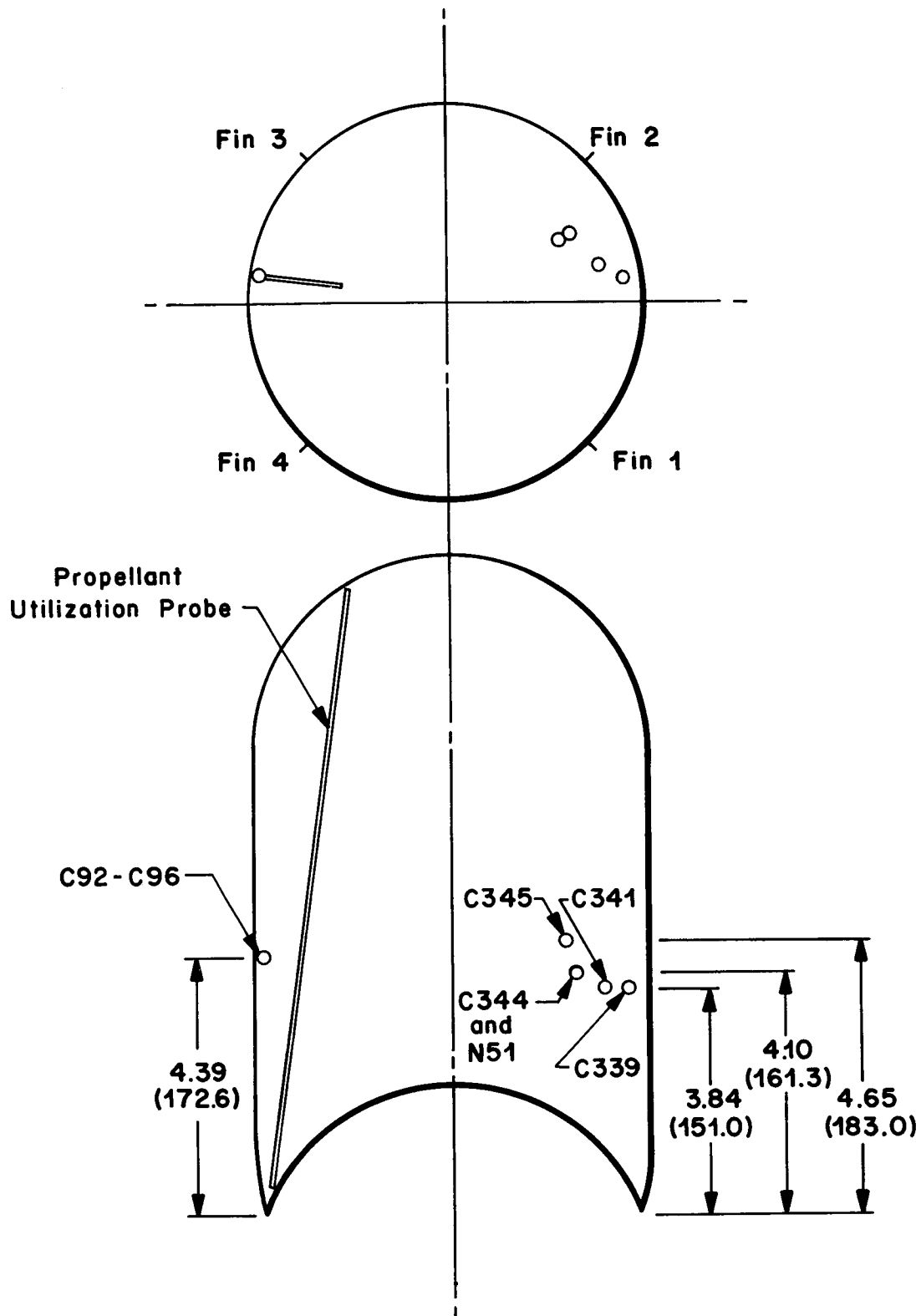


FIGURE 1. LOCATION OF THERMOCOUPLES, LIQUID-VAPOR SENSOR AND PROPELLANT UTILIZATION PROBE
ALL DIMENSIONS ARE IN METERS (INCHES)

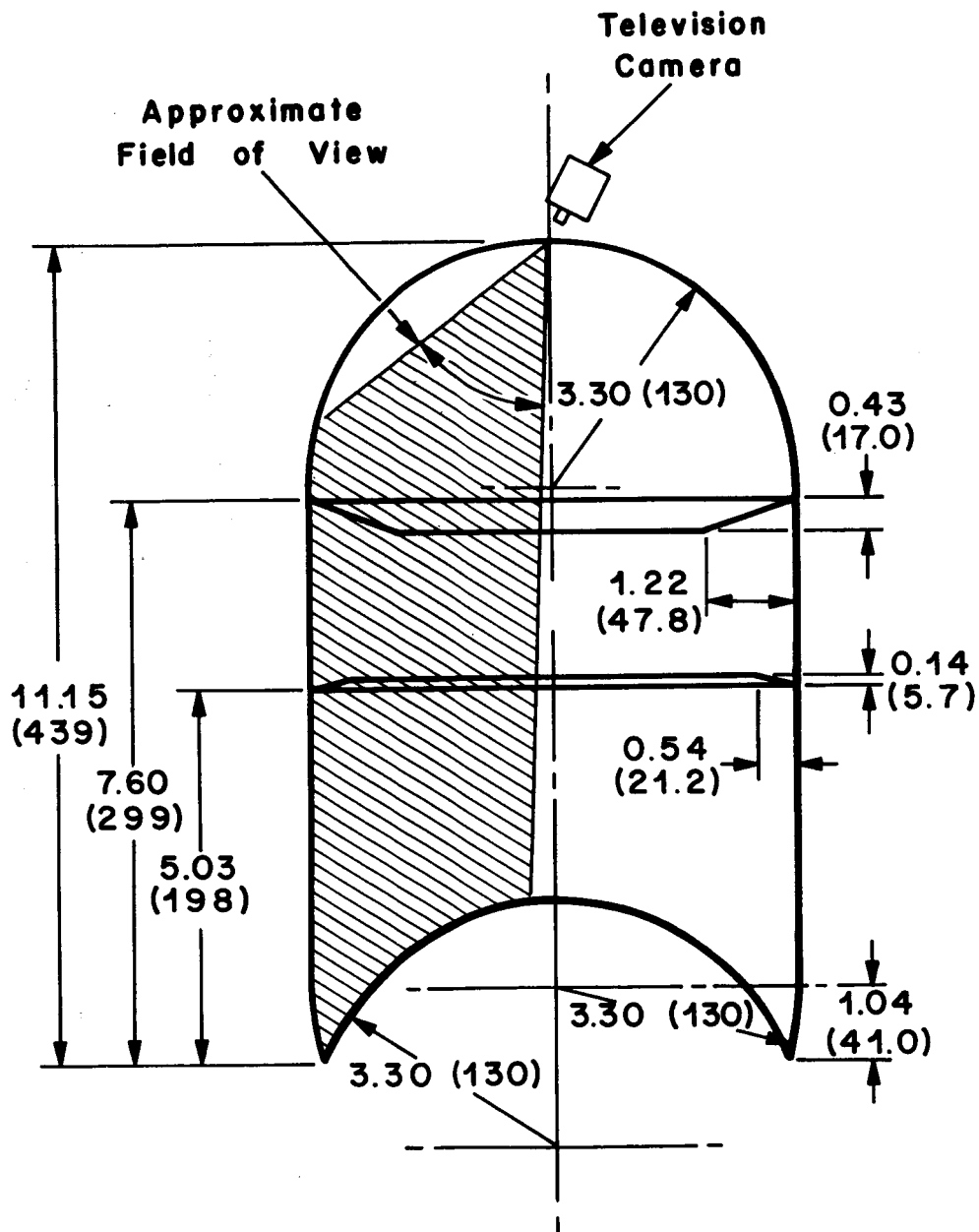


FIGURE 2. LIQUID HYDROGEN TANK DIMENSIONS
ALL DIMENSIONS ARE IN METERS (INCHES)

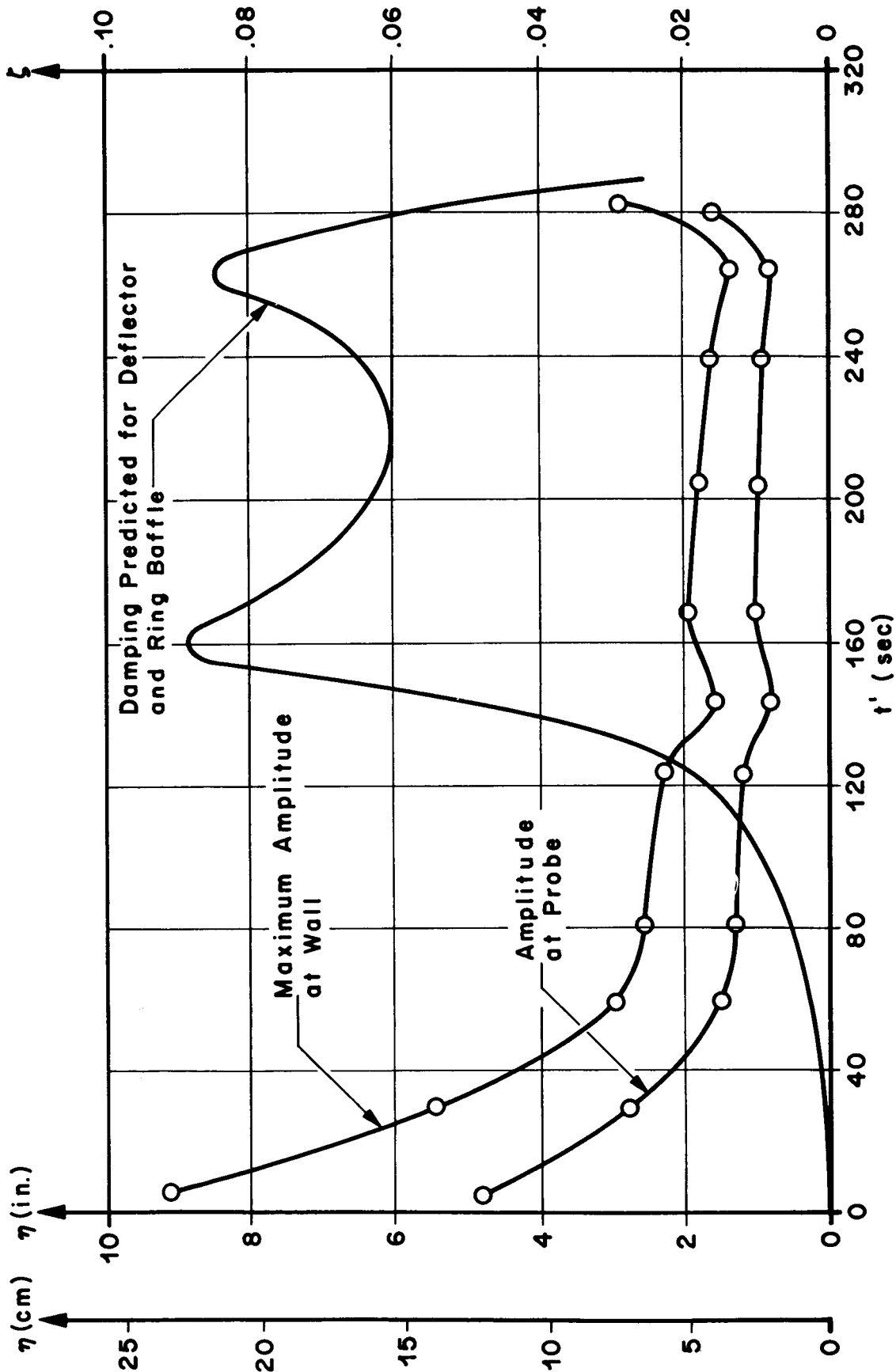


FIGURE 3. SLOSH AMPLITUDE AND PREDICTED DAMPING DURING SECOND STAGE BURN

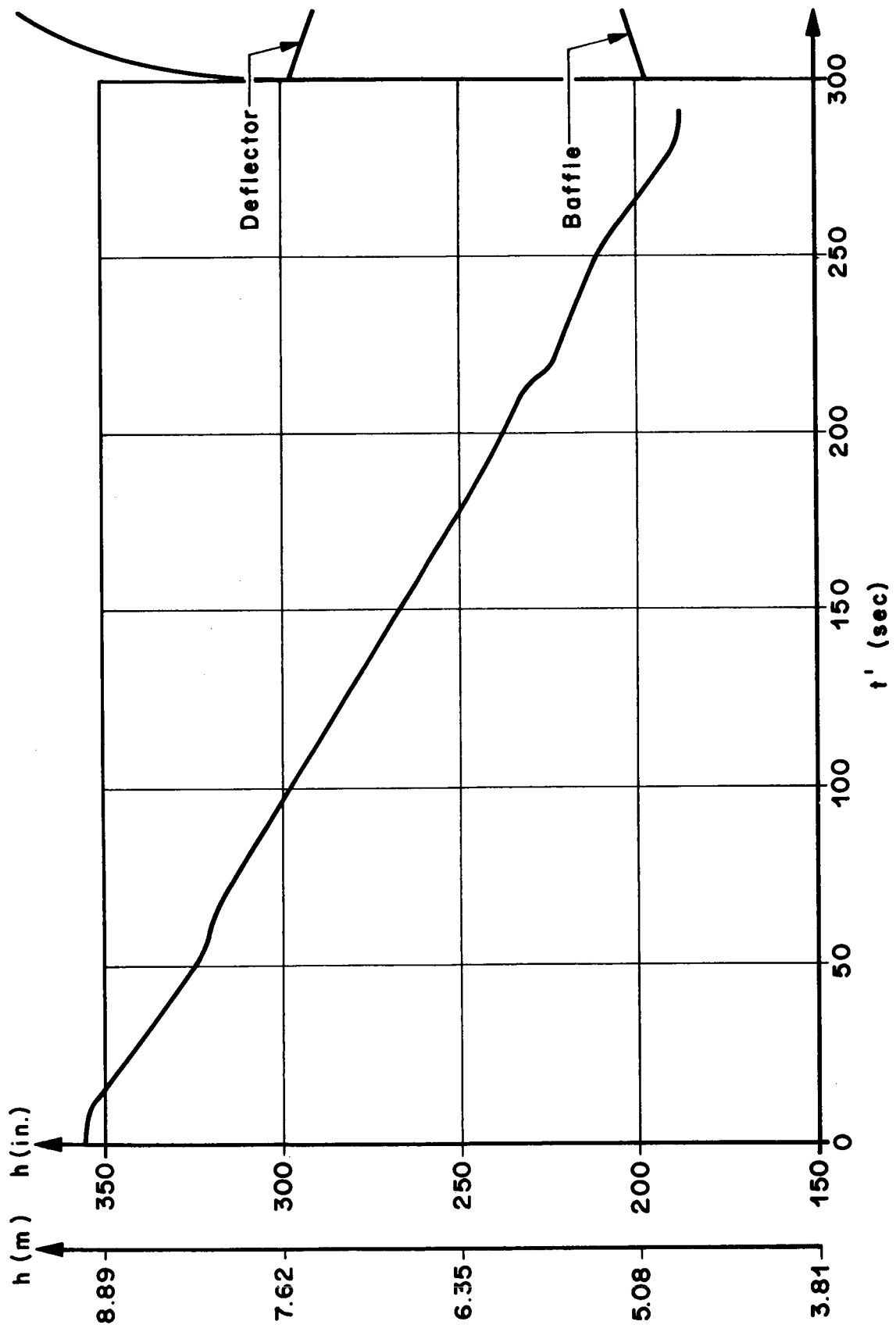


FIGURE 4. LIQUID HYDROGEN LEVEL DURING SECOND STAGE BURN

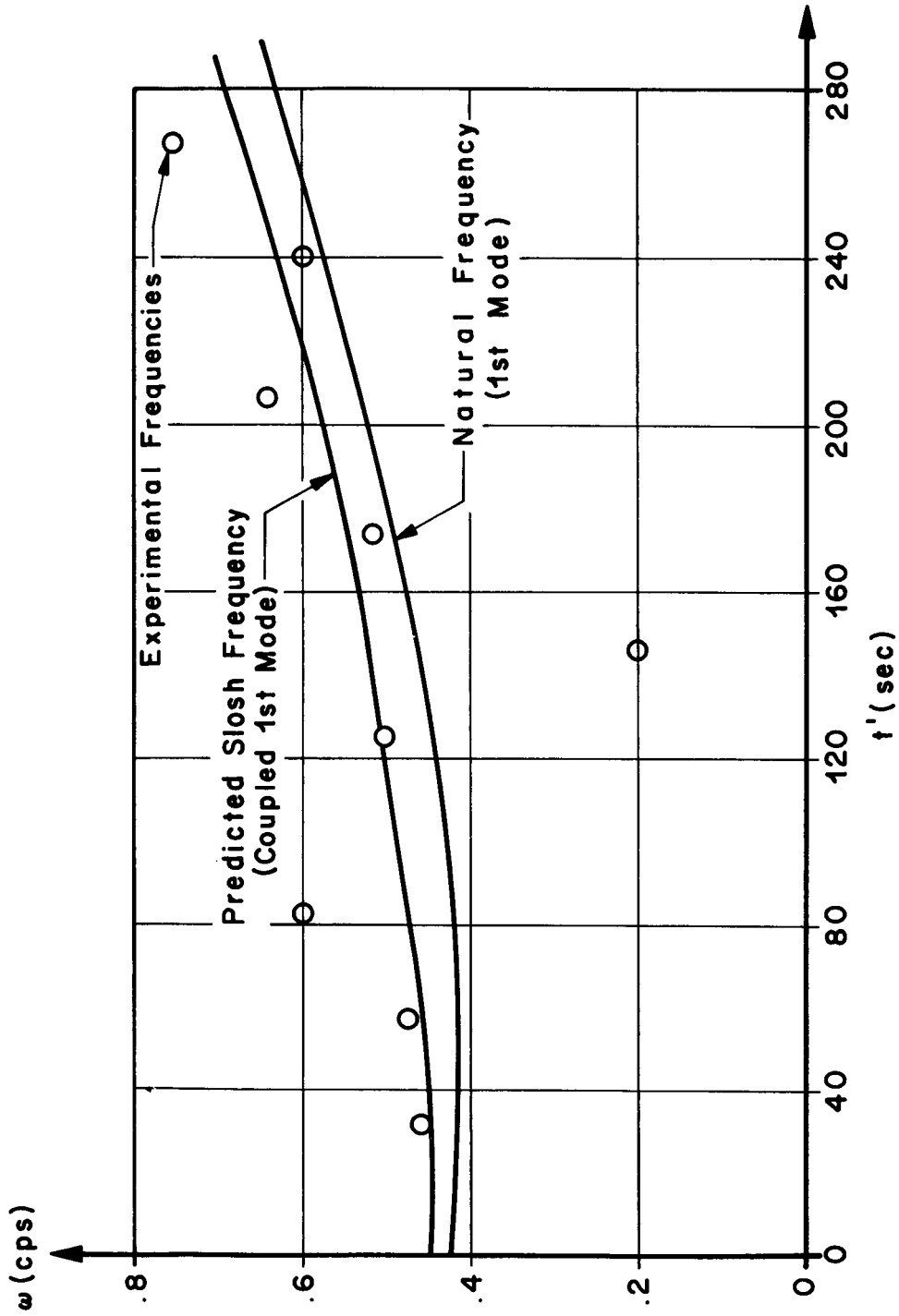


FIGURE 5. SLOSHING FREQUENCIES DURING SECOND STAGE BURN

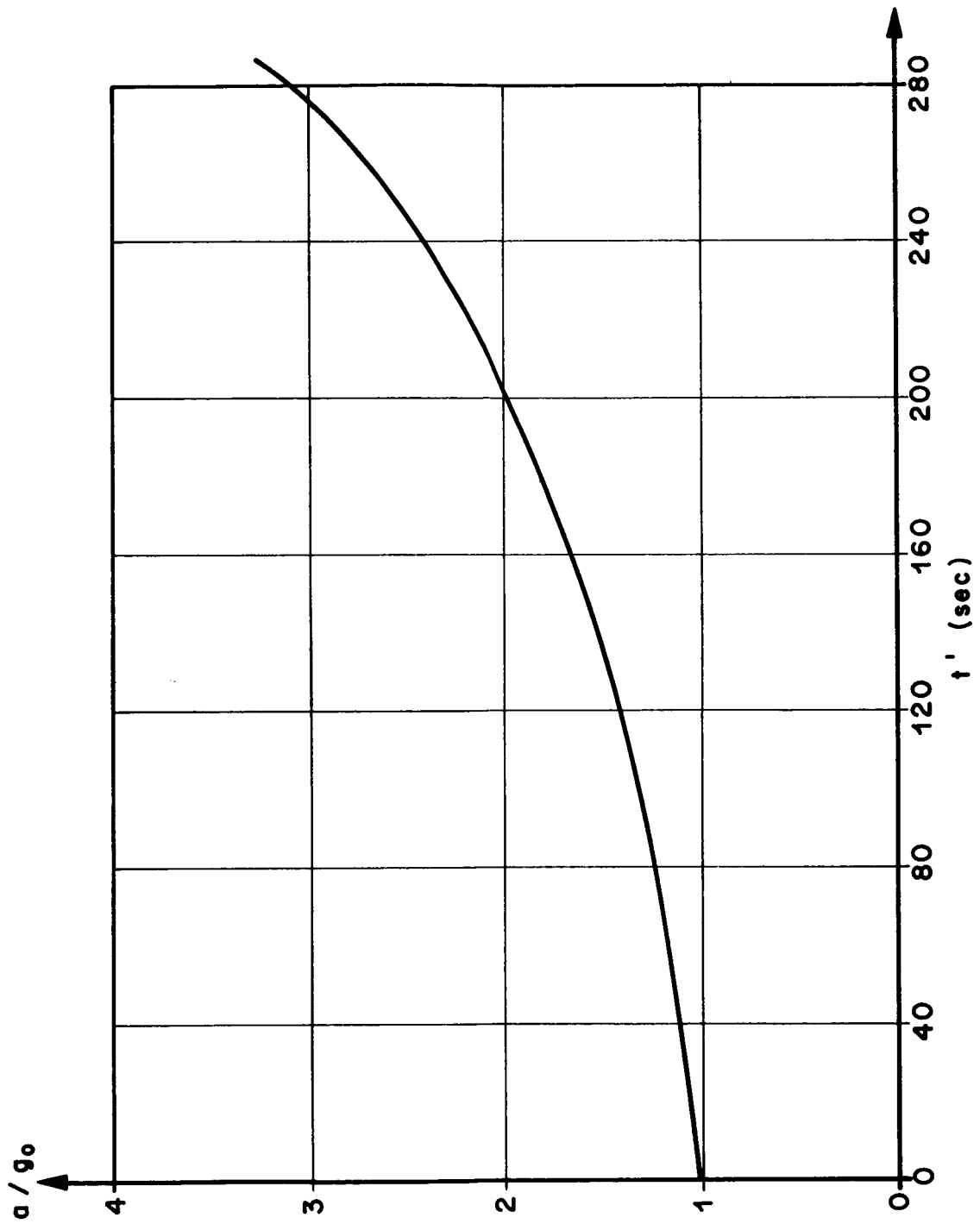
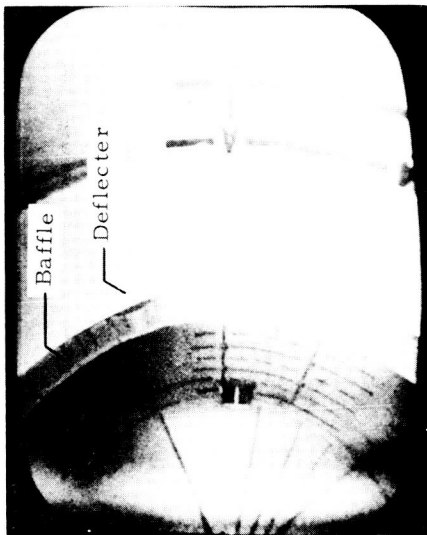


FIGURE 6. ACCELERATION DURING SECOND STAGE BURN

t = 442



t = 422



t = 495



t = 474

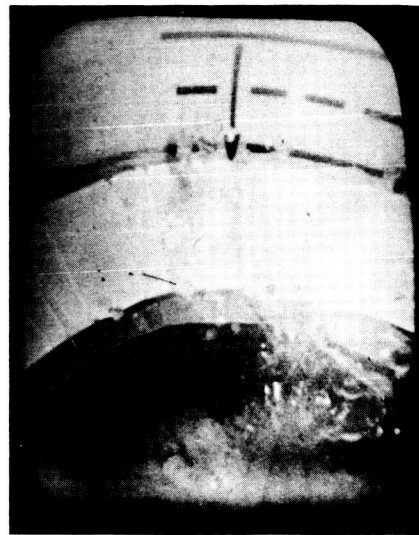


FIGURE 7. PROPELLANT DYNAMICS AT SECOND STAGE CUTOFF

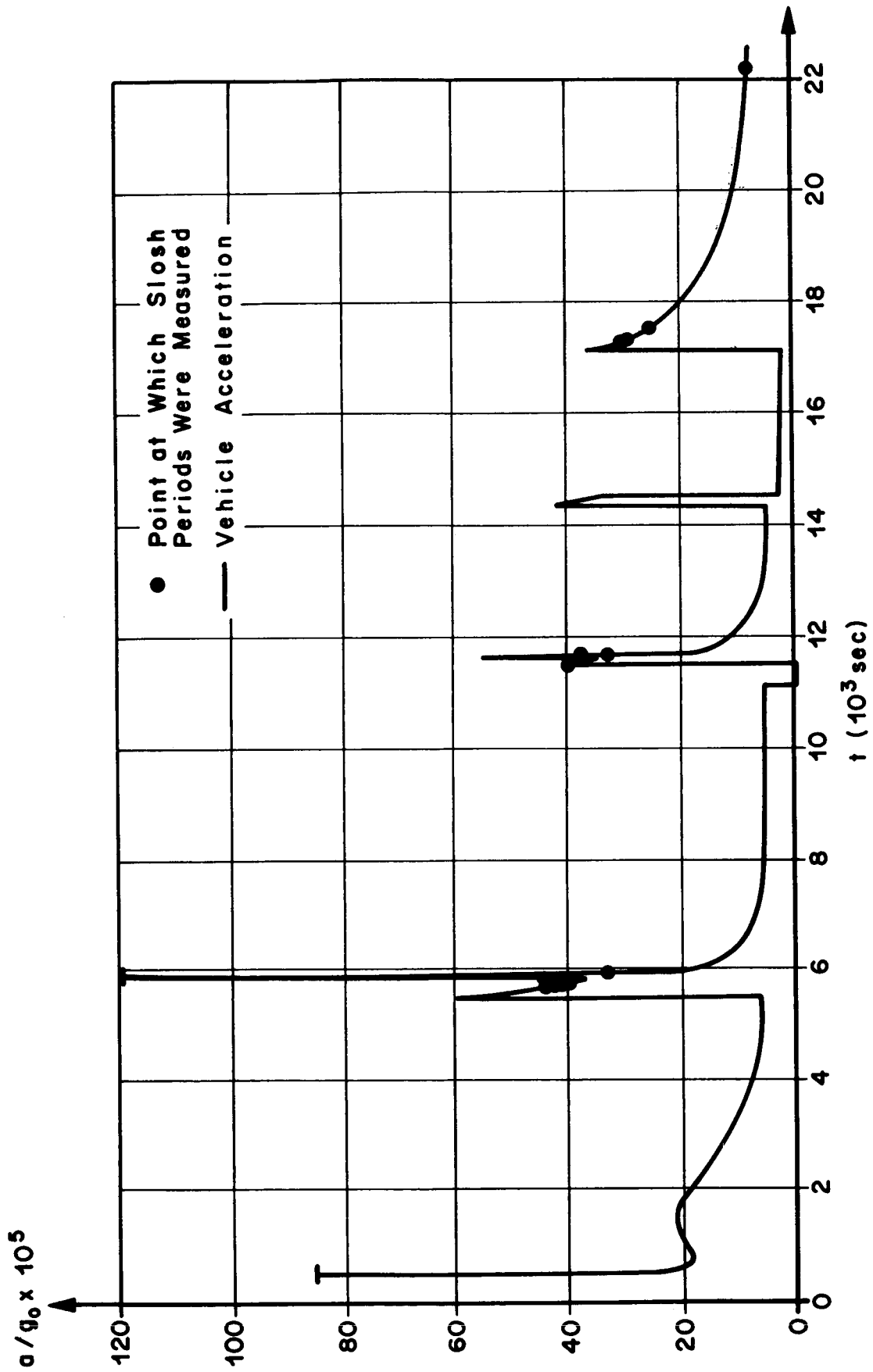


FIGURE 8. ACCELERATIONS DURING ORBIT

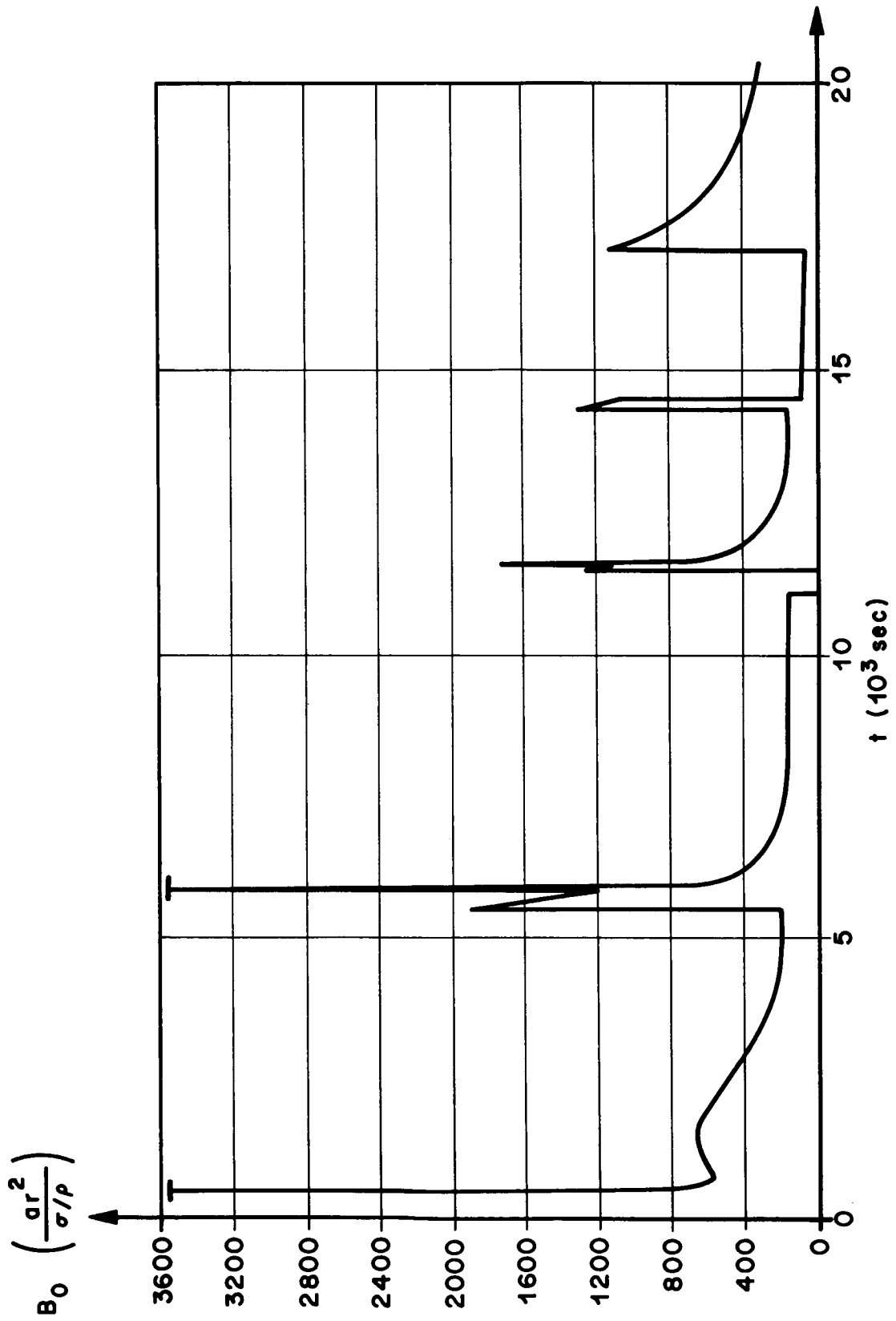


FIGURE 9. BOND NUMBERS DURING ORBIT

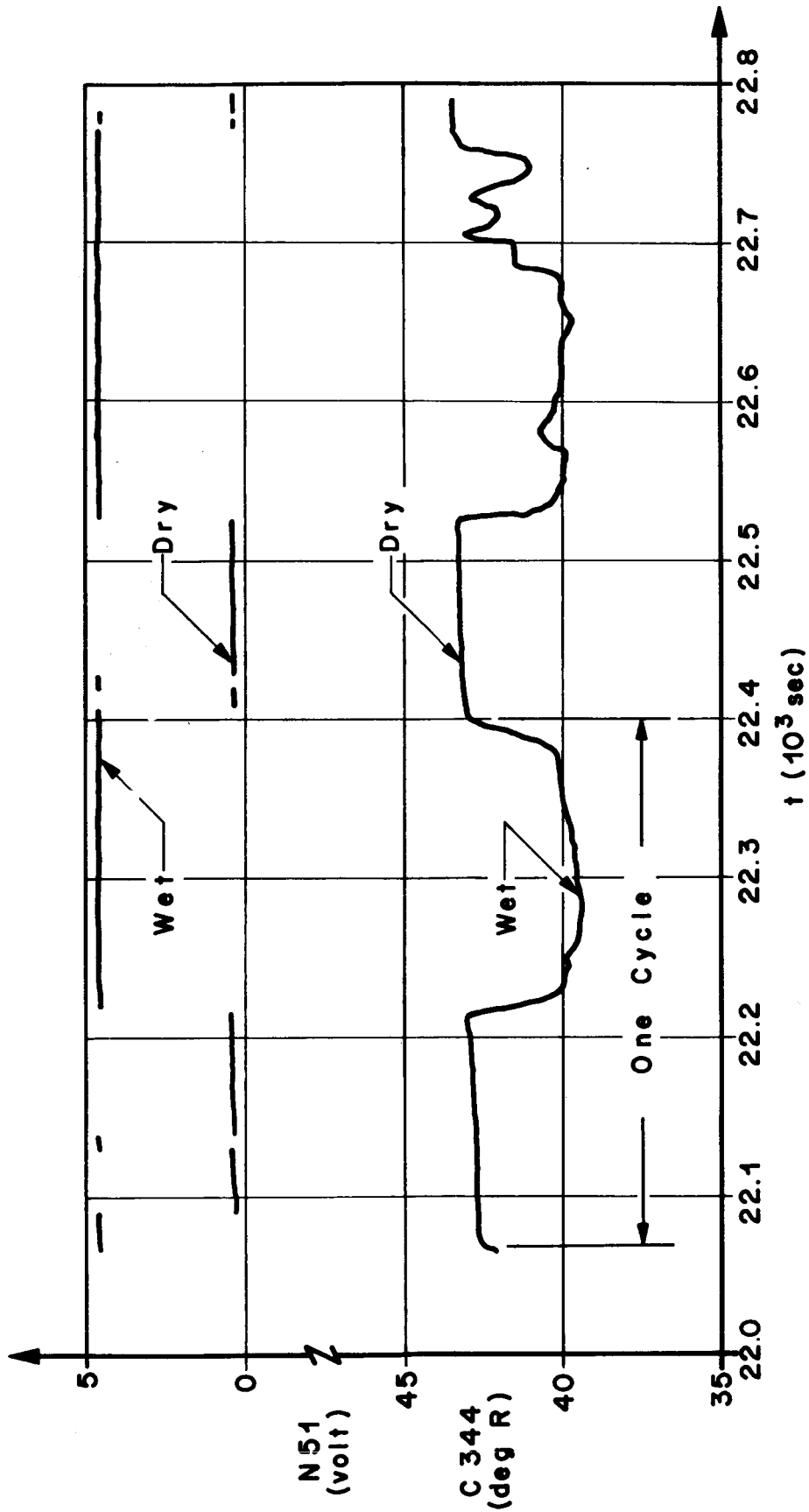


FIGURE 10. COMPARISON OF LIQUID VAPOR SENSOR AND THERMOCOUPLE READINGS AT ONE LOCATION

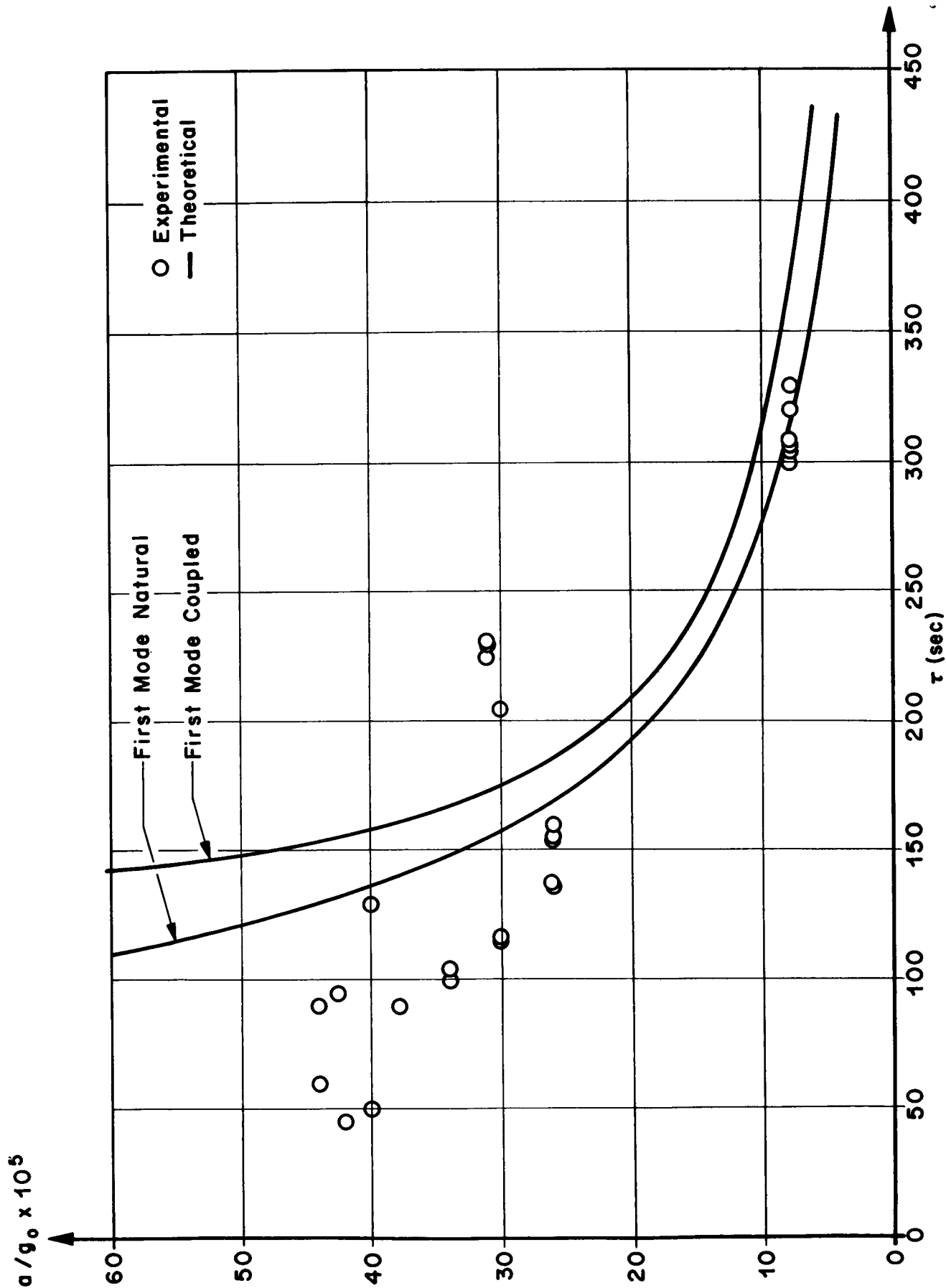


FIGURE 11. COMPARISON OF EXPERIMENTAL AND PREDICTED SLOSH PERIODS IN ORBIT

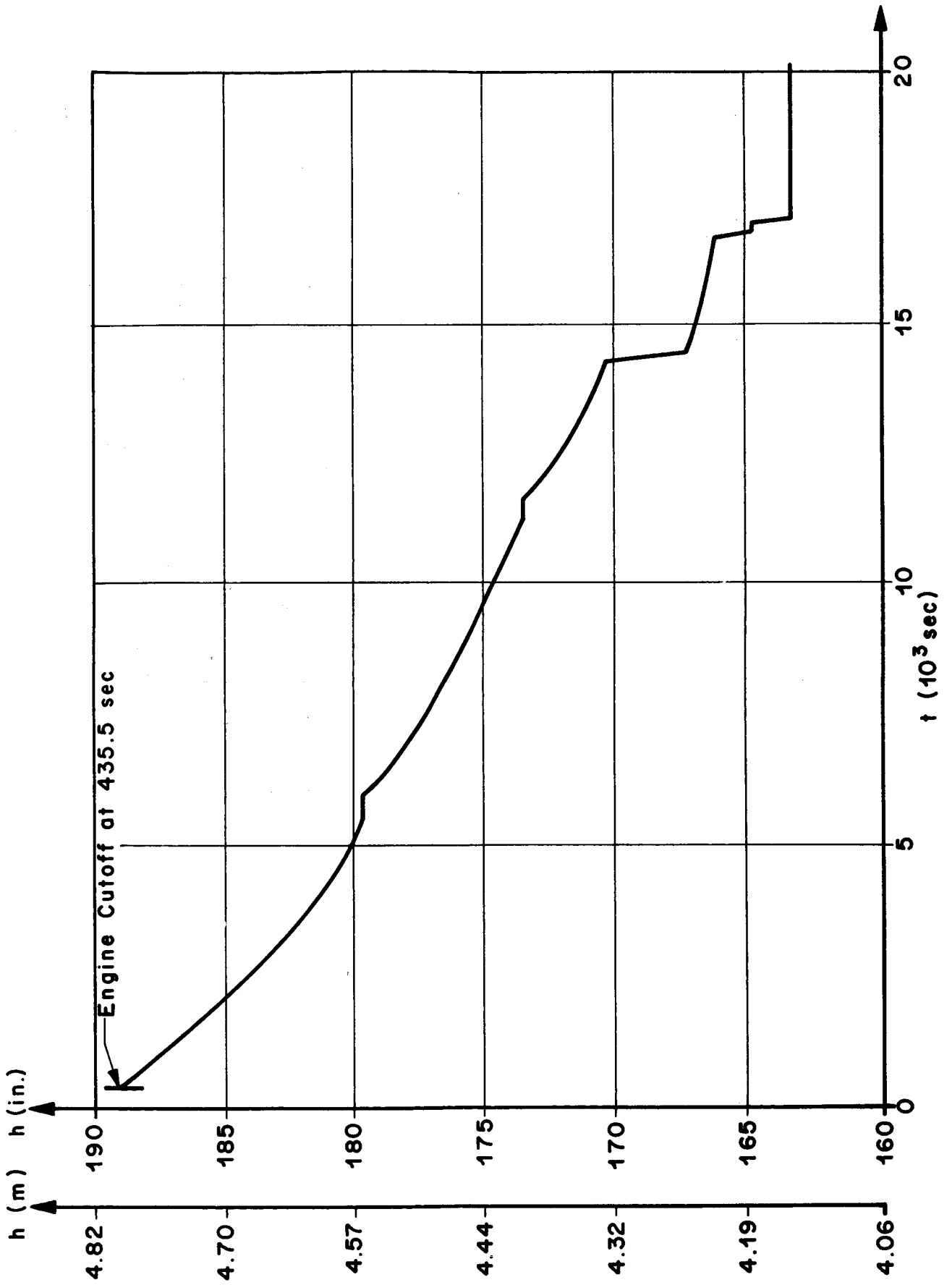


FIGURE 12. PROPELLANT LEVEL IN TANK DURING ORBIT

REFERENCES

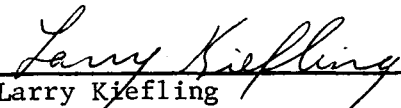
1. Satterlee, H. M. and W. C. Reynolds, "The Dynamics of the Free Liquid Surface in Cylindrical Containers Under Strong Capillary and Weak Gravity Conditions," Stanford University Technical Report LG-2, 1964.
2. Reynolds, W. C., M. A. Saad and H. M. Satterlee, "Capillary Hydrostatics and Hydrodynamics at Low g," Stanford University Technical Report LG-3, 1964.
3. Benedikt, E. T., "A Study of Propellant Behavior at Zero Gravity," North American Aviation Report SID 66-286, 1966.
4. Fung, F. C. W., "Dynamic Response of Liquids in Partially Filled Containers Suddenly Experiencing Weightlessness," Cornell Aeronautical Laboratory Report No. AG-1995-S-1, 1965.
5. Swalley, F. E., G. K. Platt and L. J. Hastings, "Saturn V Low-Gravity Fluid Mechanics Problems and Their Investigation by Full-Scale Orbital Experiment," Proceedings of a Symposium on Fluid Mechanics and Heat Transfer Under Low Gravity held Palo Alto, California, 1965.
6. Minutes of AS-203 First General Evaluation Meeting, Memo R-AERO-F-135-66, July 15, 1966 Marshall Space Flight Center, Confidential.
7. Minutes of AS-203 Summary Meeting No. 2, R-AERO-F-154-66, August 8, 1966, Marshall Space Flight Center, Confidential.
8. Lomen, D. O., "Digital Analysis of Liquid Propellant Sloshing in Mobile Tanks with Rotational Symmetry," General Dynamics Technical Report GD/A-DDE64-062, 1964.
9. Ryan, R. S. and H. Buchannan, "An Evaluation of the Low-g Propellant Behavior of a Space Vehicle During Waiting Orbit," NASA TM X-53476, 1966.

ORBITAL INVESTIGATION OF PROPELLANT DYNAMICS
IN A LARGE ROCKET BOOSTER

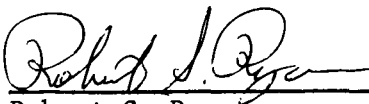
by H. J. Buchanan and F. M. Bugg

The information in this report has been reviewed for security classification. Review of any information concerning Department of Defense or Atomic Energy Commission programs has been made by the MSFC Security Classification Officer. This report, in its entirety, has been determined to be unclassified.

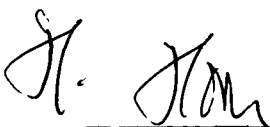
This document has also been reviewed and approved for technical accuracy.



Larry Kiefling
Chief, Structural Dynamics Section



Robert S. Ryan
Chief, Dynamics Analysis Branch



Helmut J. Horn
Chief, Dynamics and Flight Mechanics Division



E. D. Geissler
Director, Aero-Astroynamics Laboratory

DISTRIBUTION

DEP-T

R-ASTR

Dr. Haeussermann
Mr. Hosenthien
Mr. B. Moore
Mr. Blackstone
Mr. Mink
Mr. Clark
Mr. Seltzer
Mr. Fisher
Mr. Nicaise

R-P&VE

Dr. Lucas
Mr. Hellebrand
Mr. Showers
Mr. Paul
Mr. Wood
Mr. Platt
Mr. Hastings
Mr. Swalley
Mr. Lifer

MS-IP

MS-IPL (8)

MS-H

I-RM-M

CC-P

R-AERO

Dr. Geissler
Mr. Horn
Mr. Dahm
Mr. Lindberg
Mr. Baker
Mr. W. Vaughan
Mr. Thomae
Mr. Ryan
Dr. McDonough
Mr. Rheinfurth
Mr. T. Deaton
Mr. Hagood
Mr. Townsend
Mr. Kiefling

R-AERO (Cont'd)

Mr. Swift
Mr. Buchanan (10)
Mr. Milner
Mr. Hays
Mr. Worley
Mr. Pack
Mr. Bugg (10)
Mr. Muller
Mr. Papadopoulos
Mr. Billups
Mrs. King
Mr. Stone

MS-T (6)

Sci. & Tech. Info. Facility (25)
P. O. Box 33
College Park, Maryland
Attn: NASA Rep. (S-AK/RKT)

Chrysler Corp. Space Div.
New Orleans, La.
Attn: R. Wells

The Boeing Co.
304 Oakwood Ave., N. E.
Huntsville, Ala. 35801
Attn: G. Riley

Douglas Aircraft Co.
DAC-MSFC
Bldg. 4481, Rm. 41
Attn: Mr. Paul Dixon

Langley Research Center
Langley Sta., Hampton, Va.
Attn: Mr. Stephens, Mail Stop 244

Chrysler Corp.
HIC Bldg., Huntsville
Dept. 4812
Attn: Mr. Kavanaugh